Electronic Supplementary Material (ESI) for Energy & Environmental Science.
This journal is © The Royal Society of Chemistry 2015

# Holistic design guidelines for solar hydrogen production by photo-electrochemical routes

## (Electronic Supplementary Information)

**Mikael Dumortier[1], Saurabh Tembhurne[1], Sophia Haussener[1,*]**

[1]Laboratory of Renewable Energy Science and Engineering, EPFL, Station 9, 1015 Lausanne, Switzerland
*Corresponding author: sophia.haussener@epfl.ch

## Model development

The performance of the PEC device was assessed by modeling the performance of the photoabsorbers (i.e. PV) and the membrane-separated electrocatalysts (i.e. PEMEC) by equivalent circuits. The operating current was determined by ensuring simultaneous fulfillment of the current-voltage characteristics of the photoabsorbers and the membrane-separated electrocatalysts.[1]

### *II.1 Performance model of the photovoltaics*

Two different PV cells were considered: *i*) III-V cells (GaInP/GaAs) representing high-performing and high-cost cells, and *ii*) Si-based cells representing low-cost, low performance cells. Isothermal operation at $T$ = 298 K was assumed for both PV cells at all irradiation concentrations. The AM1.5 spectrum distribution was considered as the incoming non-concentrated irradiation spectrum and was weighed with the 2093 kWh m$^{-2}$ yr$^{-1}$ yearly-averaged direct normal irradiation (DNI) of Sevilla in southern Spain for tracked concentrating devices while the 1872 kWh m$^{-2}$ yr$^{-1}$ global horizontal irradiation (GHI) was used for untracked non-concentrating devices. This represents a 77% and 69%, respectively, of the 2716 kWh m$^{-2}$ yr$^{-1}$ total yearly-averaged irradiation at this location.[2] The performance of the multi-junction GaInP/GaAs PV was assumed constant for concentrations ranging from 1 to 1000 suns, with a fill factor of 85%, close to an ideal behavior.[3] The open-circuit characteristics of GaInP/GaAs tandem cells (band gaps 1.9 eV and 1.43 eV)[4] were the Shockley-Queisser limits.[5] Current-voltage behavior of GaInP/GaAs PV cells was modeled by the ideal diode equation:

$$i = i_{\mathrm{sc}} - i_{\mathrm{rec}}\left(e^{F_{\mathrm{F}}V/RT} - 1\right). \tag{i}$$

The dark current $i_{\mathrm{rec}}$ was calculated as:

$$i_{\mathrm{rec}} = i_{\mathrm{sc}} e^{-F_{\mathrm{F}}V_{\mathrm{oc}}/RT}. \tag{ii}$$

The maximum STH efficiency (based on the $i_{\mathrm{sc}}$ and the total irradiation of 2716 kWh m$^{-2}$ yr$^{-1}$) was 12 % considering the efficiency of the concentrator (which is initially 85 %). The maximum STH efficiency for the non-concentrated case was 12.6 %.

The short current behavior of a-Si/µc-Si/µc-Si PV cells was obtained by a phenomenological correlation combining two sets of reported experimental values.[6,7] The resulting current-voltage characteristics were given as (with $\phi_{\mathrm{ref}}$ = 223 W m$^{-2}$):

$$\frac{i}{i_{\mathrm{sc}}} = 1 + f - f\left(1 + \frac{1}{f}\right)^{\frac{V}{V_{\mathrm{oc}}}}, \tag{iii.a}$$

$$f = 10^{-5}\,\frac{C\phi}{\phi_{\mathrm{ref}}}\left(\frac{C\phi}{\phi_{\mathrm{ref}}} + 1\right). \tag{iii.b}$$

The maximum STH efficiency of this cell was 7.3% considering the efficiency of the concentrator. The maximum STH efficiency for the non-concentrated case was 7.6% considering that there is no sun tracking.

This correlation was experimentally validated for $C$ between 1 and 20 and was assumed valid for the $C$-range considered in this study. Concentration, $C$, and irradiation, $\Phi$, dependence of short circuit currents and open circuit voltages for all cells were estimated neglecting the effect of series and shunt resistances,[8]

$$i_{\mathrm{sc}}(C,\phi) = C\,\eta_{\mathrm{c}}(L)\,\eta_{\mathrm{PV}}(L)\,i_{\mathrm{sc}}(1,\phi_0)\frac{\phi}{\phi_0}, \tag{iv}$$

$$V_{\mathrm{oc}}(C,\phi) = V_{\mathrm{oc}}(1,\phi_0) + \frac{RT}{F_{\mathrm{F}}} ln\left(\frac{C\phi}{\phi_0}\right), \tag{v}$$

where $\eta_{\mathrm{c}}$ and $\eta_{\mathrm{PV}}$ are the operating time-dependent efficiencies of the concentrator and of the PV cell. $\Phi_0$ is the irradiation value at which the reference short circuit currents and open circuit voltage are calculated or measured (9 mA cm$^{-2}$ and 1.83 V for Si-based cells, 14.6 mA cm$^{-2}$ and 2.7 V for III-V cells, both at $\Phi_0$ = 1000 W m$^{-2}$).

### *II.2 Performance model of the PEM electrolyzer*

The operating voltage is the sum of the thermodynamic equilibrium potential required for the electrolysis of water at standard conditions ($V_0$ = 1.23 V) and current-dependent overpotentials generated by chemical reactions, mass and charge transport, and degradation:

$$V = V_{\mathrm{o}} + \eta_{\mathrm{ohm}} + \eta_{\mathrm{act}} + \eta_{\mathrm{conc}} + \eta_{\mathrm{degrad}}. \tag{vi}$$

The activation overpotential, $\eta_{\mathrm{act}}$, is the sum of anodic and cathodic activation overpotentials and were modeled using Tafel correlations:

$$\eta_{\mathrm{act}} = \frac{RT}{2F_{\mathrm{F}}\alpha_{\mathrm{a}}} ln\left(1 + \frac{j}{j_{0,\mathrm{a}}}\right) + \frac{RT}{2F_{\mathrm{F}}\alpha_{\mathrm{c}}} ln\left(1 + \frac{j}{j_{0,\mathrm{c}}}\right), \tag{vii}$$

with $j_{0,\mathrm{a}}$ and $j_{0,\mathrm{c}}$ being the anodic and cathodic exchange current densities, and $\alpha_{\mathrm{a}}$ = 0.85 and $\alpha_{\mathrm{c}}$ = 1 being the anodic and cathodic charge transfer coefficients.[9] A reaction overpotential of 227 mV for the Pt/$RuO_2$-based PEMEC and of 348 mV for the Ni/$Co_3O_4$-based PEMEC is required at 10 mA cm$^{-2}$.

Ohmic losses, $\eta_{\mathrm{ohm}}$, in the Nafion membrane with the thickness of $e_{\mathrm{m}}$ = 50μm and conductivity of $\sigma$ = 10 S m$^{-1}$ was modeled using:

$$\eta_{\mathrm{ohm}} = \frac{j\,e_{\mathrm{m}}}{\sigma}. \tag{viii}$$

Mass transport losses, $\eta_{\mathrm{conc}}$, were modeled using the phenomenological equation from Kim et al.:[10]

$$\eta_{\mathrm{conc}} = ae^{bj}. \tag{ix}$$

The phenomenological coefficients $a$ = 0.01 V and $b$ = 5 10$^{-4}$ m$^2$ A$^{-1}$ were fitted to experimental results given by Dedigama et al..[11] Isothermal operation at $T$ = 298 K was assumed for the PEMEC. $\eta_{\mathrm{degrad}}$ is the operating time-dependent degradation overpotential, effectively reducing the potential available for the PEMEC operation (see below for details).

### *II.3 Device operation*

The resulting operating PV cell current density, $i_{op}$, and potential was obtained by iteratively estimating the current and potential simultaneously satisfying eqs. (i) to (ix). The hydrogen mass production was calculated as:

$$\dot{m}_{H_2} = \frac{\eta_F \, i_{op} \, A_{PV} M_{H_2}}{2F_F}, \tag{x}$$

with the photoabsorber area $A_{PV}$, hydrogen molar mass $M_{H2}$ = 0.002 kg mol$^{-1}$, and Faradaic efficiency $\eta_F$ = 1. Typical current-potential performance characteristics for the two sets of PVs (Si-based and Ga-based) and PEMECs are depicted in Figure S1.

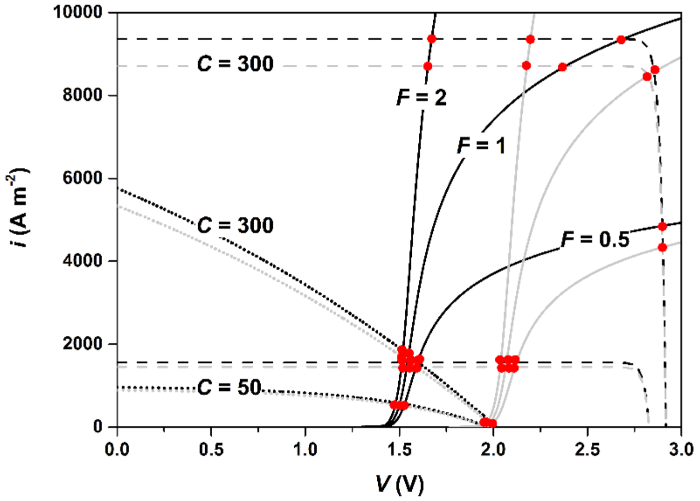

**Figure S1.** Typical current-voltage behavior of the device for varying *C* and *F*. The current is normalized by the area of the PV cell. The current density-voltage characteristic of the Ga-based cells (dashed lines) and the Si-based cells (dotted lines) are shown for *C* = 50 and 300. Pt is used as electrocatalysts in the PEMEC, for which current-voltage behavior for *F* = 0.5, 1, and 2 (solid lines) at initial operating time (black lines) or after 10 years operation (gray lines) is shown. At large *C* and small *F*, mass transport limitations in the PEMEC decrease the operating current. Operating voltages and currents are given at the intersection of the PEMEC and PV cell curves and are indicated by red dots.

## Life cycle energy and cost inventory

The energy demand per unit area has been assessed in previous work using reported data on single components, BOS not considered, and is summarized in Table 2 in the main paper text.[1] The price per unit area of components was assessed using the same method, focusing on the requirements for the manufacturing process only and excluding transportation, assembly, maintenance, and recycling of the system.

The prices of parabolic troughs and solar heliostats for tower plants have been reported to be \$295 m$^{-2}$ and \$164 m$^{-2}$.[12,13] The price of parabolic dishes and 2-axis Fresnel concentrators have been reported to be \$125 m$^{-2}$ and \$172 m$^{-2}$ for the concentrator and \$51 m$^{-2}$ and \$30 m$^{-2}$ for the tracker.[14,15] The price of Fresnel-lens-based concentrators has been reported per unit of power: The price of the concentrating module and of the tracker of the 22.7% efficient Flatcon device adds up to \$0.75 W$_p^{-1}$ resulting in a cost of \$170 m$^{-2}$.[16] The price of a 18.3 kW and 267 m$^2$ AMONIX 7700 module was reported to be \$2.9 W$^{-1}$, resulting in \$198.4 m$^{-2}$.[17] Excluding the price of the III-V cell (adjusted with the area ratio *C* = 550) and the BOS, the price of a module and tracker for this device accounted for \$138 m$^{-2}$. The energy demand per unit area for the manufacturing of the concentrating module was assessed in previous studies from reported LCAs on concentrated solar devices.[1,18–21] In this study, we averaged all the reported energy demand values to 2251 MJ $m^{-2}$ and the cost values to \$201 $m^{-2}$ for the concentrator.

For concentrating devices, yearly energy demand for tracking was estimated to be 30.9 MJ ($yr^{-1}m^{-2}$)[1] and the price \$0.9 $yr^{-1}m^{-2}$ was obtained using the electricity cost in the U.S. and a typical energy intensity of the electricity production.[22]

The price of silicon based cells has been reported to be within \$90 $m^{-2}$ to \$200 $m^{-2}$.[23,24] The mean between these values was used. The price of III-V PV cells was reported to be between \$30 000 $m^{-2}$ and \$100 000 $m^{-2}$.[14,25] We considered the latter value from the detailed report of King et al.[23] as the most reliable and conservative case and we excluded the packaging price of \$2.5 $cm^{-2}$ which was not suited for our design, resulting in a \$75 000 $m^{-2}$ price for III-V cells.

The price of PEMFC stacks has been reported to be within \$42 $m^{-2}$ to \$1000 $m^{-2}$ and resulted mostly from cost analyses on fuel cells for automotive applications.[26–33] The two major causes for price variability were the platinum load on the electrodes and the production type.[28] Price and energy demand for these PEMEC were adapted accordingly with data for electrode materials obtained from the ecoinvent database,[34] knowing that the precious metals accounted for 30% and 40% of these cost and energy demand, respectively.[35] The maximum price - \$1000 $m^{-2}$ - was chosen for the most expensive PEMEC ($RuO_2$ and Pt-based) and represented a conservative value. The price of the cheap PEMEC ($Co_3O_4$ and Ni-based) resulted in \$245 $m^{-2}$.

The price of the BOS for a generic irradiation concentration installation, its operation, maintenance, and financing was reported to be \$260 $m^{-2}$.[25] The price of the BOS for the Flatcon device was estimated to be 0.33 €$Wp^{-1}$ resulting in a total price of \$74 $m^{-2}$.[16] The sum of the energy demands of transformers, hydraulic drives, motor cables, controllers, anemometers, and sensors of the AMONIX 7700 was reported to be 550 MJ $m^{-2}$.[21] The price of the BOS was also estimated between \$40 $m^{-2}$ and \$112 $m^{-2}$ for non-concentrating devices, and the energy demand of the BOS for non-concentrating devices was estimated as 550 MJ $m^{-2}$.[22,36] The reference area for the BOS was the concentrator area. The reported price for the BOS were averaged and resulted in \$137 $m^{-2}$ for concentrating devices, \$76 $m^{-2}$ for non-concentrating ones. These averages also accounted for slightly different BOS definitions in the various studies. The averaged BOS energy demand was 550 MJ $m^{-2}$ for non-concentrating and concentrating systems.

The water needed to for the electrochemical reaction and ensuring no electrode and membrane dry out was calculated to be 86 kg $yr^{-1}m^{-2}$ (per unit area of receiver, either PV cell or concentrator).[1] The energy to produce distilled water was estimated experimentally to be 3.6 kJ $kg^{-1}$ by Moore et al.,[37] resulting in a power cost of 0.15 MJ $yr^{-1}m^{-2}$ (per unit area of concentrator) for the distilled water supply of the device. The price of the required water was assessed to be \$$1.5\cdot10^{-3}$ $yr^{-1}$ $m^{-2}$ using the price of electricity and the energy mix in the U.S.[22]

## Operating time, replacement, and degradation

The reference operating time, $L_{\mathrm{ref}}$, of the device was assumed 30 years, with all components having a replacement time of 30 years, except for the PEMEC which had a replacement time of 10 years. The degradation of the optical efficiency of the concentrator was given as:

$$\eta_{\mathrm{c}} = \eta_{\mathrm{c,0}} - G(\dot{\eta}_{\mathrm{c}}\, L, L_{\mathrm{conc}}), \tag{xi}$$

$$\eta_{\mathrm{PV}} = 1 - G(\dot{\eta}_{\mathrm{PV}}\, L, L_{\mathrm{conc}}), \tag{xii}$$

where $\eta_{c,0}$ is the initial efficiency (85%)[1] and $\dot{\eta}_{\mathrm{c}}$ the degradation rate (0.65% $yr^{-1}$). The degradation of the PV cell short circuit current was given with a similar formula with degradation rates $\dot{\eta}_{\mathrm{PV}}$ ranging from 0.17% $yr^{-1}$ to 2.5% $yr^{-1}$.[3,8] The degradation overpotential was given as:

$$\eta_{\text{degrad}} = G(\dot{\eta}_{\text{c}}\, L, L_{\text{PEMEC}}), \tag{xiii}$$

where $\dot{\eta}_{\text{c}}$ is the voltage degradation rate (1 µV h$^{-1}$ to 14 µV h$^{-1}$).[39,40] $G$ is a periodic function for every positive integer $n$ defined as $G(\dot{\eta}_{\text{ref}}, L, L_{\text{ref}}) = \dot{\eta}_{\text{ref}}\,(L - nL_{ref})$ for $nL_{\text{ref}} < L < (n+1)L_{\text{ref}}$. The performance of every device is therefore renewed after the component replacement took place.

**Additional figures**

The following figures provide additional information of optimum designs for different device types (Figures S2 and S4), the benefits of increasing the $V_{\text{oc}}$ of Si-based PV cells (Figure S3), the minimum hydrogen price and STH efficiency sensitivity of device types 2, 7, and 7* to degradation and replacement time of components (Figures S5 and S6). Figure S7 provides hydrogen energy demand, hydrogen price, and STH efficiency for the most sustainable, the most profitable and the most efficient designs at their optimum operating times.

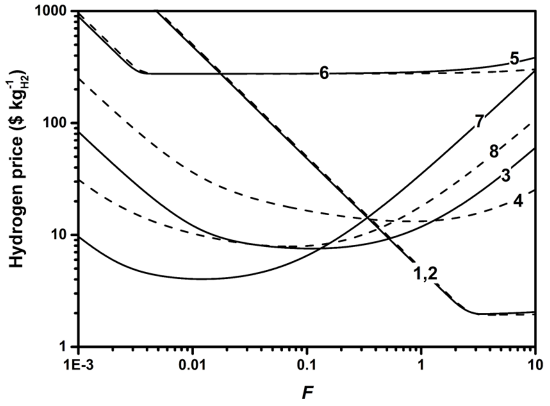

**Figure S2.** Hydrogen price as a function of current concentration, $F$, for devices 1 to 4 at $C_{\text{opt}}$, and for devices 5 to 8, at $C$ =1 using high quality (solid lines) or low cost electrocatalysts (dashed lines).

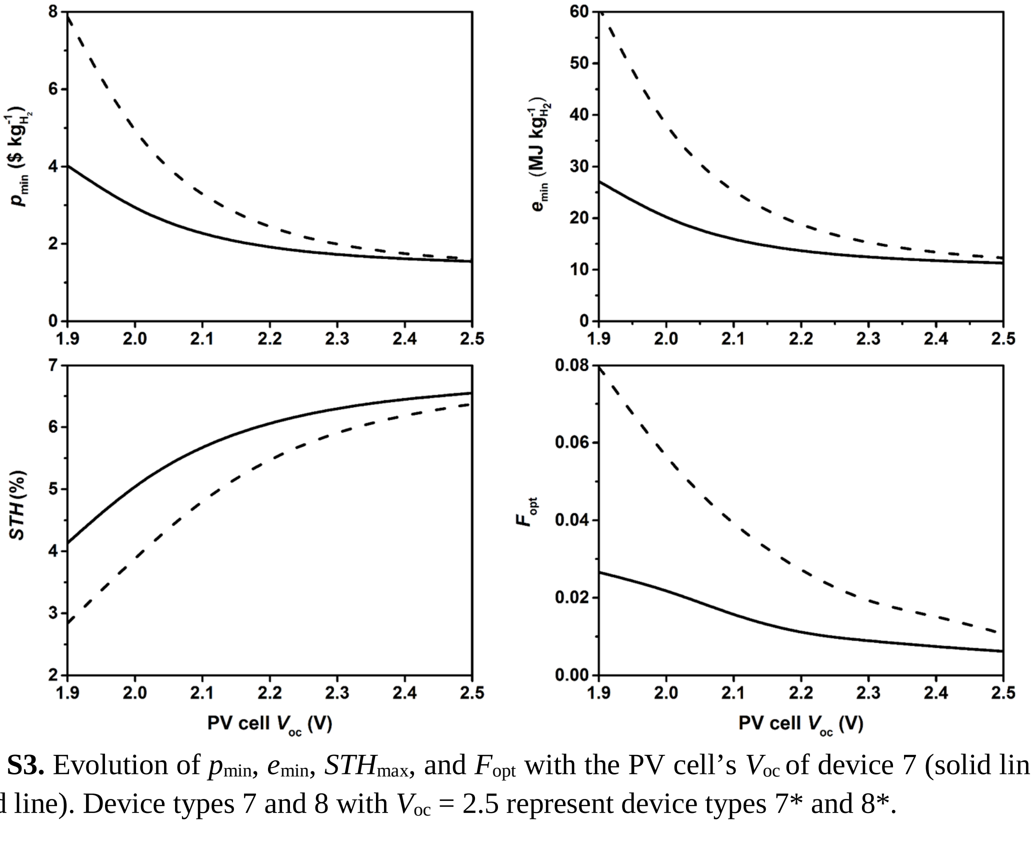

**Figure S3.** Evolution of $p_{\min}$, $e_{\min}$, $STH_{\max}$, and $F_{\text{opt}}$ with the PV cell's $V_{\text{oc}}$ of device 7 (solid line) and 8 (dashed line). Device types 7 and 8 with $V_{\text{oc}}$ = 2.5 represent device types 7* and 8*.

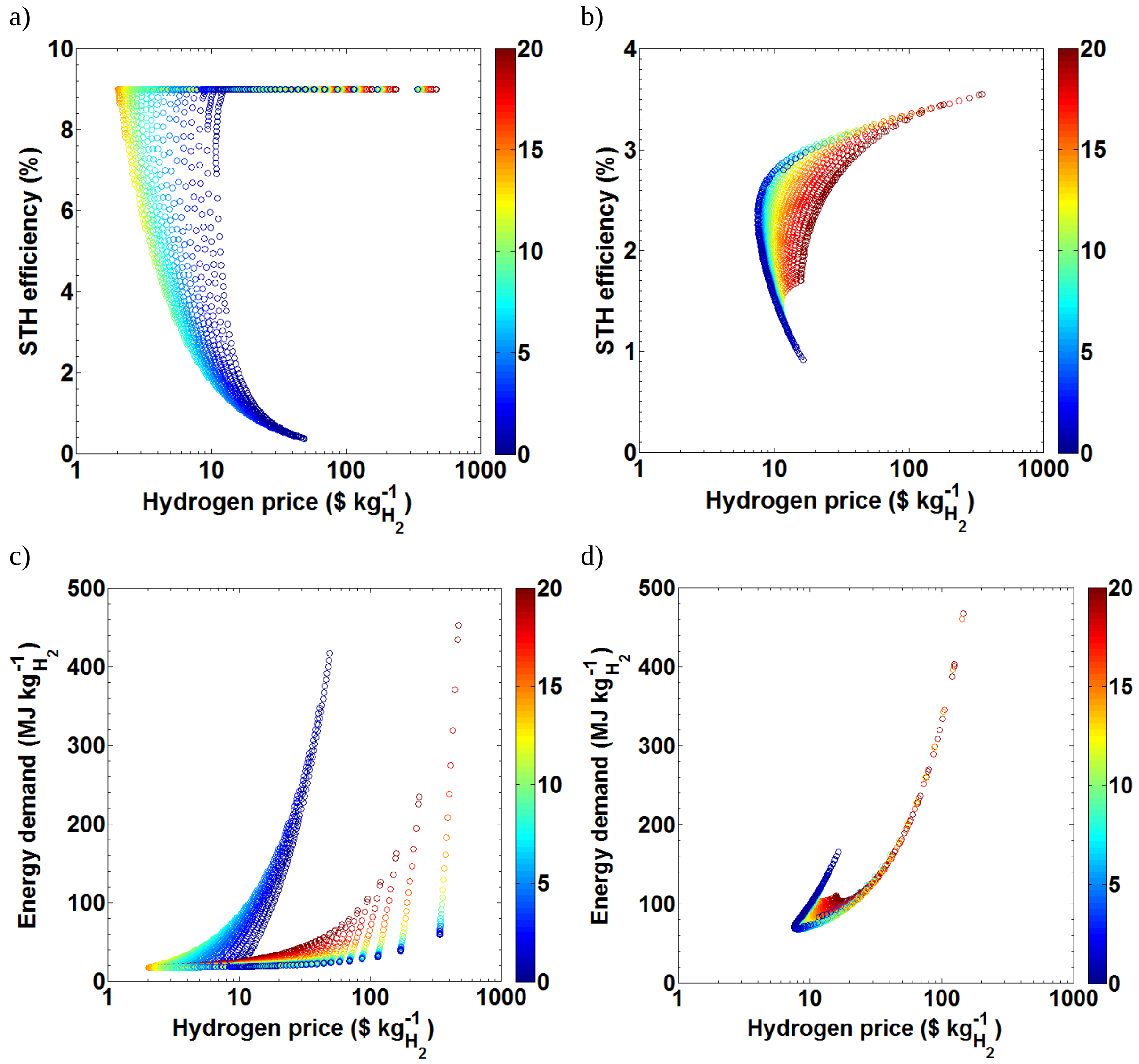

**Figure S4.** Operating time-averaged efficiency as a function of hydrogen price (a,b) and energy demand as a function of hydrogen price (c,d) for device types (a,c) 1 and (b,d) 3. The color of the points indicates a normalized current concentration ($[\log_{10}(F)+1]\cdot 10$).

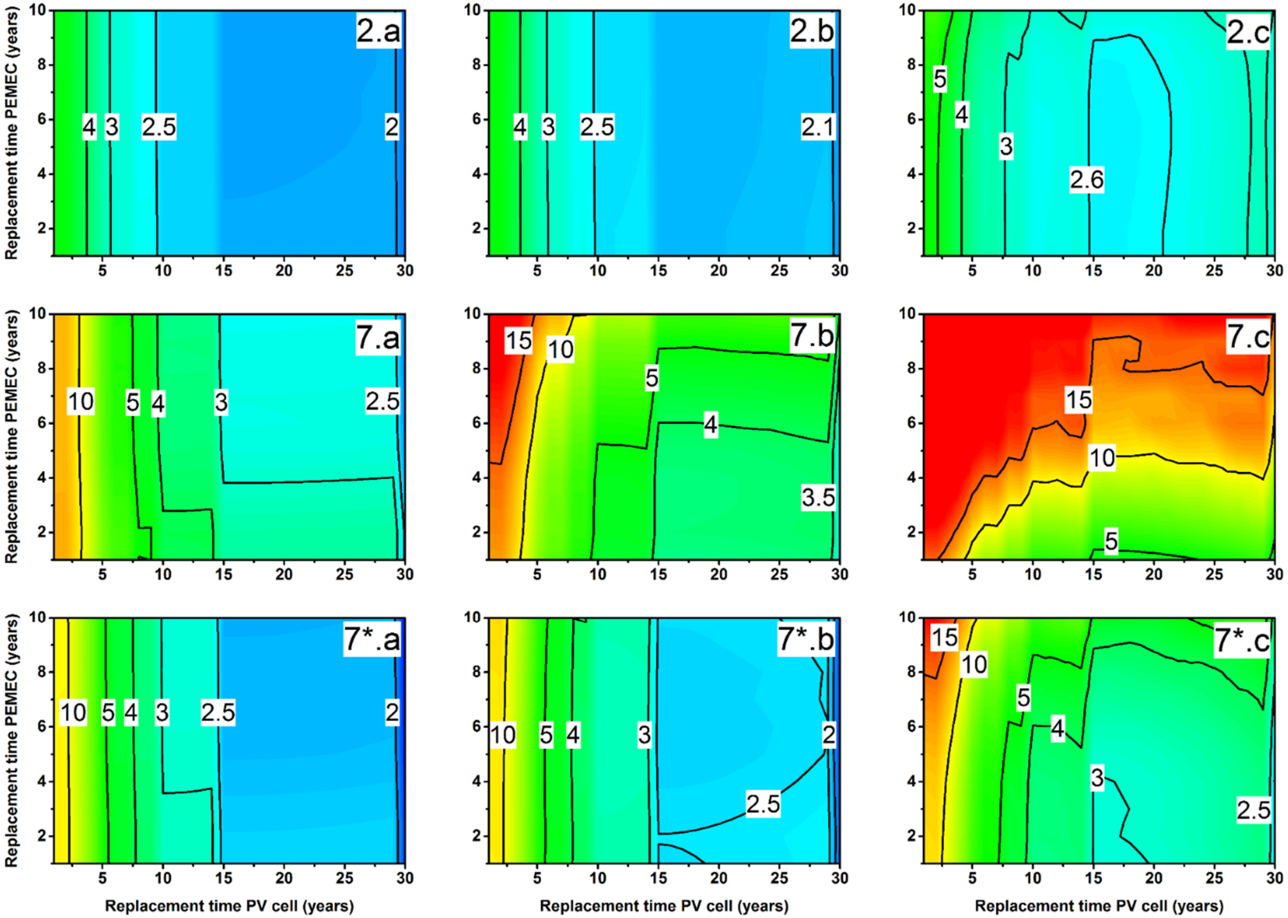

**Figure S5.** Hydrogen price $p_{\min}$ (in \$ $kg_{H2}^{-1}$) as a function of replacement time of PV cells and PEMEC for cost-optimized devices 2, 7*, and 7, for (a) optimistic, (b) reference, and (c) conservative degradation rates.

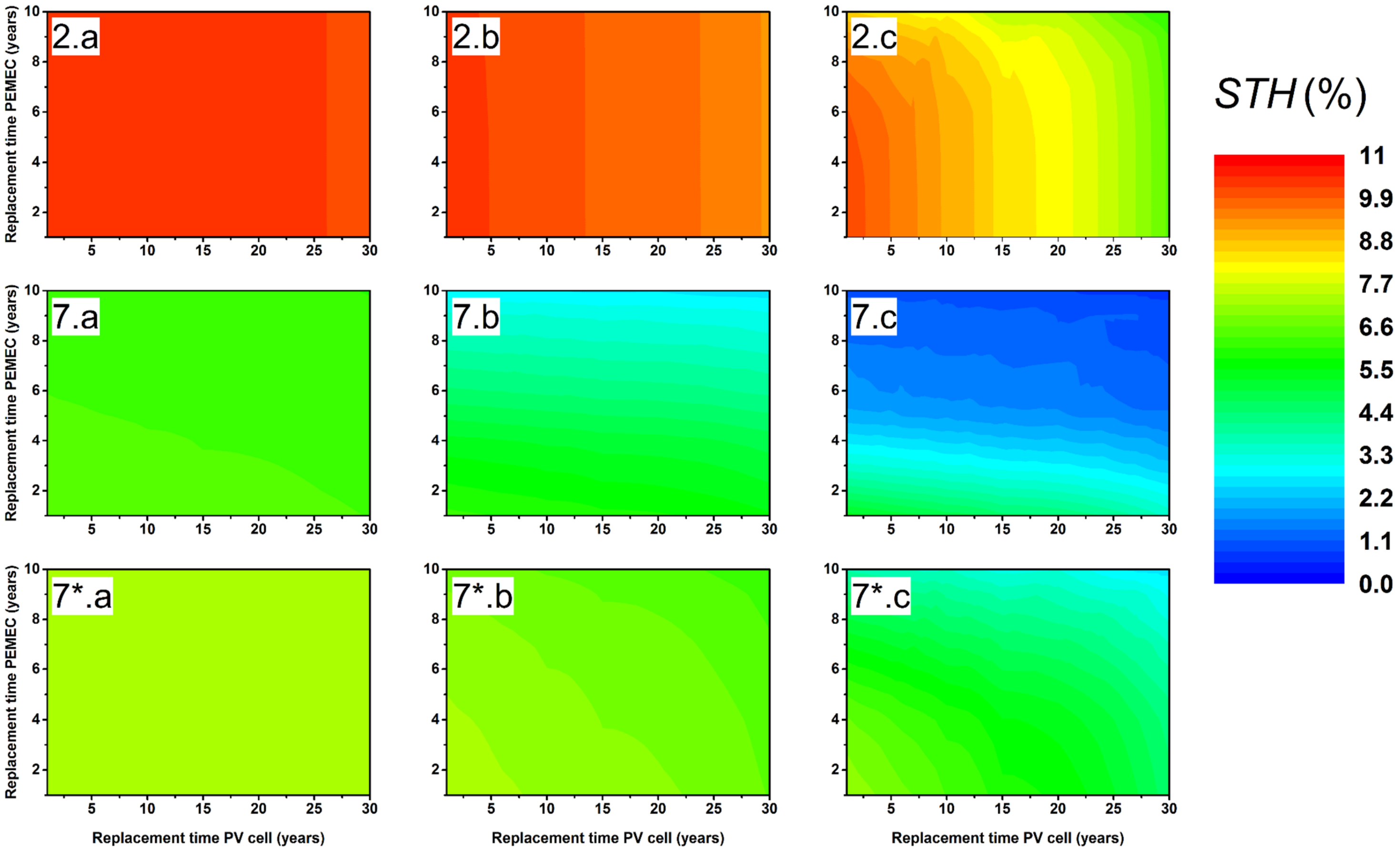

**Figure S6.** Operating time-averaged STH efficiency as a function of the replacement time of PV cells and PEMEC for cost-optimized devices 2, 7*, and 7, for (a) optimistic, (b) reference, and (c) conservative degradation rates.

| | Strategy | | | | Strategy | | | | Strategy | | | | Strategy | | |
|---|---|---|---|---|---|---|---|---|---|---|---|---|---|---|---|
| **DEVICE 1** | Min *e* | Min *p* | Max *STH* | **DEVICE 2** | Min *e* | Min *p* | Max *STH* | **DEVICE 3** | Min *e* | Min *p* | Max *STH* | **DEVICE 4** | Min *e* | Min *p* | Max *STH* |
| *C* | 1000 | 1000 | 1000 | *C* | 980 | 1000 | 1000 | *C* | 6 | 7 | 1 | *C* | 7 | 9 | 1 |
| *F* | 3.2 | 3.2 | 10 | *F* | 3.2 | 3.2 | 10 | *F* | 0.25 | 0.12 | 10 | *F* | 0.74 | 0.74 | 10 |
| $e$ (MJ $kg_{H2}^{-1}$) | 16.9 | 16.9 | 17.2 | $e$ (MJ $kg_{H2}^{-1}$) | 16.9 | 16.9 | 17.1 | $e$ (MJ $kg_{H2}^{-1}$) | 67.3 | 69.6 | 1064.4 | $e$ (MJ $kg_{H2}^{-1}$) | 129.6 | 130.1 | 1089.8 |
| $p$ (\$ $kg_{H2}^{-1}$) | 2.0 | 2.0 | 2.1 | $p$ (\$ $kg_{H2}^{-1}$) | 2.0 | 2.0 | 2.0 | $p$ (\$ $kg_{H2}^{-1}$) | 8.1 | 7.5 | 348.1 | $p$ (\$ $kg_{H2}^{-1}$) | 13.2 | 13.2 | 128.3 |
| *STH* (%) | 9.0 | 9.0 | 9.0 | *STH* (%) | 9.0 | 9.0 | 9.0 | *STH* (%) | 2.6 | 2.4 | 3.5 | *STH* (%) | 1.4 | 1.4 | 2.5 |
| **DEVICE 5** | Min *e* | Min *p* | Max *STH* | **DEVICE 6** | Min *e* | Min *p* | Max *STH* | **DEVICE 7** | Min *e* | Min *p* | Max *STH* | **DEVICE 8** | Min *e* | Min *p* | Max *STH* |
| *F* | 0.1 | 0.1 | 10 | *F* | 0.1 | 0.1 | 10 | *F* | 0.027 | 0.013 | 10 | *F* | 0.066 | 0.066 | 10 |
| $e$ (MJ $kg_{H2}^{-1}$) | 37.2 | 37.2 | 363.3 | $e$ (MJ $kg_{H2}^{-1}$) | 36.2 | 36.2 | 264.5 | $e$ (MJ $kg_{H2}^{-1}$) | 27.1 | 27.8 | 882.5 | $e$ (MJ $kg_{H2}^{-1}$) | 61.0 | 61.0 | 905.8 |
| $p$ (\$ $kg_{H2}^{-1}$) | 280.8 | 280.8 | 391.4 | $p$ (\$ $kg_{H2}^{-1}$) | 280.0 | 280.0 | 307.1 | $p$ (\$ $kg_{H2}^{-1}$) | 4.3 | 4.0 | 295.9 | $p$ (\$ $kg_{H2}^{-1}$) | 7.9 | 7.9 | 107.8 |
| *STH* (%) | 10.9 | 10.9 | 10.9 | *STH* (%) | 10.9 | 10.9 | 10.9 | *STH* (%) | 2.9 | 2.6 | 4.1 | *STH* (%) | 1.4 | 1.4 | 2.8 |
| **DEVICE 9** | Min *e* | Min *p* | Max *STH* | **DEVICE 10** | Min *e* | Min *p* | Max *STH* | **DEVICE 11** | Min *e* | Min *p* | Max *STH* | **DEVICE 12** | Min *e* | Min *p* | Max *STH* |
| *C* | 340 | 400 | 310 | *C* | 320 | 380 | 270 | *C* | 14 | 28 | 1 | *C* | 9 | 11 | 1 |
| $e$ (MJ $kg_{H2}^{-1}$) | 17.0 | 17.7 | 17.0 | $e$ (MJ $kg_{H2}^{-1}$) | 17.0 | 17.7 | 17.0 | $e$ (MJ $kg_{H2}^{-1}$) | 71.5 | 75.6 | 180.6 | $e$ (MJ $kg_{H2}^{-1}$) | 129.7 | 130.2 | 244.2 |
| $p$ (\$ $kg_{H2}^{-1}$) | 2.7 | 2.6 | 2.8 | $p$ (\$ $kg_{H2}^{-1}$) | 2.7 | 2.6 | 2.9 | $p$ (\$ $kg_{H2}^{-1}$) | 9.7 | 8.9 | 46.9 | $p$ (\$ $kg_{H2}^{-1}$) | 13.3 | 13.2 | 27.6 |
| *STH* (%) | 9.0 | 8.6 | 9.0 | *STH* (%) | 9.0 | 8.6 | 9.0 | *STH* (%) | 2.5 | 2.2 | 3.2 | *STH* (%) | 1.4 | 1.4 | 1.9 |
| **DEVICE 13** | Min *e* | Min *p* | Max *STH* | **DEVICE 14** | Min *e* | Min *p* | Max *STH* | **DEVICE 15** | Min *e* | Min *p* | Max *STH* | **DEVICE 16** | Min *e* | Min *p* | Max *STH* |
| $e$ (MJ $kg_{H2}^{-1}$) | 69.1 | 69.1 | 69.1 | $e$ (MJ $kg_{H2}^{-1}$) | 58.5 | 58.5 | 58.5 | $e$ (MJ $kg_{H2}^{-1}$) | 115.8 | 115.8 | 115.8 | $e$ (MJ $kg_{H2}^{-1}$) | 100.7 | 100.7 | 100.7 |
| $p$ (\$ $kg_{H2}^{-1}$) | 291.6 | 291.6 | 291.6 | $p$ (\$ $kg_{H2}^{-1}$) | 282.6 | 282.6 | 282.6 | $p$ (\$ $kg_{H2}^{-1}$) | 35.7 | 35.7 | 35.7 | $p$ (\$ $kg_{H2}^{-1}$) | 18.3 | 18.3 | 18.3 |
| *STH* (%) | 10.9 | 10.9 | 10.9 | *STH* (%) | 10.9 | 10.9 | 10.9 | *STH* (%) | 3.7 | 3.7 | 3.7 | *STH* (%) | 2.2 | 2.2 | 2.2 |
| **DEVICE 3*** | Min *e* | Min *p* | Max *STH* | **DEVICE 4*** | Min *e* | Min *p* | Max *STH* | **DEVICE 7*** | Min *e* | Min *p* | Max *STH* | **DEVICE 8*** | Min *e* | Min *p* | Max *STH* |
| *C* | 5 | 6 | 1 | *C* | 5 | 5 | 1 | *C* | 1 | 1 | 1 | *C* | 1 | 1 | 1 |
| *F* | 0.046 | 0.032 | 10 | *F* | 0.08 | 0.08 | 10 | *F* | 0.0062 | 0.0043 | 10 | *F* | 0.011 | 0.011 | 10 |
| $e$ (MJ $kg_{H2}^{-1}$) | 32.4 | 32.6 | 683.7 | $e$ (MJ $kg_{H2}^{-1}$) | 35.4 | 35.4 | 502.3 | $e$ (MJ $kg_{H2}^{-1}$) | 11.3 | 11.4 | 557.1 | $e$ (MJ $kg_{H2}^{-1}$) | 12.3 | 12.3 | 404.1 |
| $p$ (\$ $kg_{H2}^{-1}$) | 3.4 | 3.3 | 223.6 | $p$ (\$ $kg_{H2}^{-1}$) | 3.6 | 3.6 | 59.1 | $p$ (\$ $kg_{H2}^{-1}$) | 1.6 | 1.5 | 186.8 | $p$ (\$ $kg_{H2}^{-1}$) | 1.6 | 1.6 | 48.1 |
| *STH* (%) | 5.0 | 4.9 | 5.5 | *STH* (%) | 4.6 | 4.6 | 5.4 | *STH* (%) | 6.2 | 6.1 | 6.6 | *STH* (%) | 5.8 | 5.8 | 6.4 |
| **DEVICE 11*** | Min *e* | Min *p* | Max *STH* | **DEVICE 12*** | Min *e* | Min *p* | Max *STH* | **DEVICE 15*** | Min *e* | Min *p* | Max *STH* | **DEVICE 16*** | Min *e* | Min *p* | Max *STH* |
| *C* | 19 | 38 | 1 | *C* | 14 | 16 | 1 | *C* | 1 | 1 | 1 | *C* | 1 | 1 | 1 |
| $e$ (MJ $kg_{H2}^{-1}$) | 37.1 | 38.7 | 105.6 | $e$ (MJ $kg_{H2}^{-1}$) | 39.4 | 39.5 | 88.1 | $e$ (MJ $kg_{H2}^{-1}$) | 66.2 | 66.2 | 66.2 | $e$ (MJ $kg_{H2}^{-1}$) | 51.9 | 51.9 | 51.9 |
| $p$ (\$ $kg_{H2}^{-1}$) | 4.7 | 4.4 | 27.4 | $p$ (\$ $kg_{H2}^{-1}$) | 4.0 | 4.0 | 10.0 | $p$ (\$ $kg_{H2}^{-1}$) | 20.4 | 20.4 | 20.4 | $p$ (\$ $kg_{H2}^{-1}$) | 6.3 | 6.3 | 6.3 |
| *STH* (%) | 4.7 | 4.2 | 5.5 | *STH* (%) | 4.4 | 4.3 | 5.3 | *STH* (%) | 6.5 | 6.5 | 6.5 | *STH* (%) | 6.2 | 6.2 | 6.2 |

**Figure S7.** Irradiation concentration, *C*, current concentration, *F*, hydrogen energy requirements, *e*, hydrogen price, *p*, and operating time-averaged *STH*, for the most sustainable (Min *e*), the most profitable (Min *p*), and the most efficient (Max *STH*, averaged over 30 years operational time) designs of device types 1 to 16 and devices 3*, 4*, 7*, 8*, 11*, 12* 15* and 16*. Minimum *p* and *e* are reached for operating time between 27 and 30 years operational time. Grey color indicates a constrained *C* or *F*.

## References

1 M. Dumortier and S. Haussener, *Energy Environ. Sci.*, 2015, DOI: 10.1039/C5EE01269D.

2 Geo Solar Model, *Solar Resource Overview*, 2014. SolarGIS report SG-0000-0000-1, SolarGIS, Bratislava, Slovakia, 2014.

3 T. Cooper, M. Pravettoni, M. Cadruvi, G. Ambrosetti and A. Steinfeld, *Sol. Energy Mater. Sol. Cells*, 2013, **116**, 238–251.

4 N. J. Mohr, J. J. Schermer, M. A. J. Huijbregts, A. Meijer and L. Reijnders, *Prog. Photovoltaics Res. Appl.*, 2007, **15**, 163–179.

5 W. Shockley and H. J. Queisser, *J. Appl. Phys.*, 1961, **32**, 510–519.

6 L. M. van Dam, W. G. J. H. van Sark, Proceedings of the 2011 MRS Spring Meeting, San Francisco, 2011.

7 K. Söderström, G. Bugnon, R. Biron, C. Pahud, F. Meillaud, F.-J. Haug and C. Ballif, *J. Appl. Phys.*, 2012, **112**, 114503–114507.

8 A. Luque and S. Hegedus, *Handbook of photovoltaic science and engineering*, Wiley, Hoboken, USA, 2003.

9 J. O. Bockris, A. Ammar and S. Huq, *J. Phys. Chem*, 1957, **61**, 879–886.

10 J. Kim, S. Lee, S. Srinivasan and C. E. Chamberlin, *J. Electrochem. Soc.*, 1995, **142**, 2670–2674.

11 I. Dedigama, K. Ayers, P. R. Shearing and D. J. L. Brett, *Int. J. Electrochem. Sci.*, 2014, **9**, 2662–2681.

12 C. Turchi, M. Mehos, C. K. Ho, and G. J. Kolb, Presented at SolarPACES 2010, Perpignan, September, 2010.

13 G. J. Kolb, S. a Jones, M. W. Donnelly, D. Gorman, R. Thomas, R. Davenport, and R. Lumia, *Heliostat Cost Reduction Study*, Sandian report SAND2007-3, Sandia National Laboratories, Oak Ridge, TN, 2007.

14 S. Kurtz, *Opportunities and Challenges for Development of a Mature Concentrating Photovoltaic Power Industry Opportunities and Challenges for Development of a Mature Concentrating Photovoltaic Power Industry*, NREL report NREL/TP-5200-43208, National Renewable Energy Laboratory, Golden, Colorado, 2012

15 R. M. Swanson, *Prog. Photovoltaics Res. Appl.*, 2000, **8**, 93–111.

16 H. Lerchenmüller, A. W. Bett, J. Jaus, and G. Willeke, presented at *International Conference on Solar Concentrators for the Generation of Electricity or Hydrogen*, Scottsdale, Arizona, 2005.

17 R. Stevenson, *Compd. Semicond.*, **19**, 2013, 18–19.

18 P. Krishnamurthy and R. Banerjee, Lecture Notes in Information Technology, 2012, **9**, pp. 509–514.

19 J. P. Caballero, Undergraduate thesis project, Universidad Carlos III de Madrid and Università degli studi de Perugia, 2012.

20 G. Peharz, F. Dimroth and H. P. V System, *Prog. Photovoltaics Res. Appl.*, 2005, **13**, 627–634.

21 V. M. Fthenakis and H. C. Kim, *Prog. photovoltaics*, 2013, **21**, 379–388.

22 J. Mason and K. Zweibel, in *Solar Hydrogen Generation*, eds. K. Rajeshwar, R. McConnell, and S. Licht, Springer, New York, 2008, vol. 1, pp. 273–313.

23 M. Taylor, *Cost Analysis of Solar Photovoltaics*, IRENA working paper, International Renewable Energy Agency, 2012.

24 B. A. Pinaud, J. D. Benck, L. C. Seitz, A. J. Forman, Z. Chen, T. G. Deutsch, B. D. James, K. N. Baum, G. N. Baum, S. Ardo, H. Wang, E. Miller and T. F. Jaramillo, *Energy Environ. Sci.*, 2013, **6**, 1983–2002.

25 R. R. King, D. Bhusari, D. Larrabee, X. Liu, E. Rehder, K. Edmondson, H. Cotal, R. K. Jones, J. H. Ermer, C. M. Fetzer, D. C. Law and N. H. Karam, *Prog. photovoltaics*, 2012, **20**, 801–815.

26 C. Rodriguez, M. Modestino, D. Psaltis, and C. Moser, *Energy Environ. Sci.*, 2014, **7**, 3828–3835.

27 Autostack, *PEMFC Stack Manufacturing Cost Estimation*, Public summary of FCH-JU Project #: 245142, 2010.

28 F. Simbolotti, *Fuel cells*, IEA Energy Technol. Essentials, 2007, 1–4.

29 S. Satyapal, M. Mills, S. Byham, Z. Hou, and N. Kee Suk, *Fuel Cell Cost Analysis Summary Based on a study conducted during 2007 and 2008 among contributing members of the International Partnership for Hydrogen and Fuel Cells in the Economy*, IPHE working report, International Partnership for Hydrogen and Fuel cells in the Economy, Washington, DC, 2008.
30 J. Sinha, J. Marcinkoski, *Cost Analyses of Fuel Cell Stacks/Systems*, DOE Hydrogen Program, FY 2010 Annual Progress Report, Department of Energy, Washington, DC, 2010
31 J. Spendelow and J. Marcinkoski, *DOE Fuel Cell Technologies Program Record*, Department of Energy, Washington, DC, 2010.
32 H. Tsuchiya, *Int. J. Hydrogen Energy*, 2004, **29**, 985–990.
33 S. Lasher and P. Kopf, *Direct Hydrogen PEMFC Manufacturing Cost Estimation for Automotive Applications Fuel Cell Tech Team Review*, TIAX LLC working report, Cambridge, MA, 2008..
34. Ecoinvent V3.0, Swiss Center for Life Cycle Inventories, 2013.
35 M. Pehnt, *Int. J. Hydrogen Energy*, 2001, **26**, 91–101.
36 J. M. Mason, V. M. Fthenakis, T. Hansen and H. C. Kim, *Prog. Photovoltaics Res. Appl.*, 2006, **14**, 179–190.
37 B. A. Moore, E. Martinson and D. Raviv, *Desalination*, 2008, **220**, 502–505.
38. D. C. Jordan and S. R. Kurtz, *Prog. Photovoltaics Res. Appl.*, 2013, **21**, 12–29.
39. J. Wu, X. Z. Yuan, J. J. Martin, H. Wang, J. Zhang, J. Shen, S. Wu, and W. Merida, *J. Power Sources*, 2008, **184**, 104–119.
40. X.-Z. Yuan, S. Zhang, H. Wang, J. Wu, J. C. Sun, R. Hiesgen, K. A. Friedrich, M. Schulze, A. Haug, and J. Colin, *J. Power Sources*, 2010, **195**, 7594–7599.